

## Inhibition Effect of Tangerine Peel Extract on J55 Steel in CO<sub>2</sub>-saturated 3.5 wt. % NaCl Solution

Shuliang Wang<sup>1</sup>, Bensong Wu<sup>1</sup>, Lanlan Qiu<sup>1,2</sup>, Yuyao Chen<sup>1</sup>, Jing Yuan<sup>1</sup>, Songsong Chen<sup>1</sup>, Mingyu Bao<sup>1</sup>, Chunyan Fu<sup>1,\*</sup>, Xin Wang<sup>1,\*</sup>

<sup>1</sup> School of Materials Science and Engineering, Southwest Petroleum University, 8 Xindu Avenue, Chengdu, Sichuan 610500, China

<sup>2</sup> College of Materials Science and Engineering, Chongqing University, Chongqing 400044, China

\*E-mail: [wsliang1465@126.com](mailto:wsliang1465@126.com), [xin.wang@swpu.edu.cn](mailto:xin.wang@swpu.edu.cn)

Received: 7 August 2017 / Accepted: 21 September 2017 / Published: 12 November 2017

Corrosion inhibition effect of a natural plant product, tangerine peel extract or TPE, on J55 steel in CO<sub>2</sub>-saturated 3.5 wt. % NaCl solution was investigated. The results show that TPE is a good mixed type green inhibitor in the test solution. Inhibition efficiency was found to increase with the increase of the inhibitor concentration while decrease as the temperature increases. Adsorption behavior study of the TPE on J55 steel shows that it is a spontaneous physical process where a monolayer was eventually formed on the steel surface. The adsorption characteristics are also demonstrated and found to meet with the Langmuir isothermal absorption model and the El-Awady dynamic model.

**Keywords:** Corrosion inhibitor, Tangerine peel extract, J55 steel, CO<sub>2</sub> corrosion

### 1. INTRODUCTION

Carbon dioxide (CO<sub>2</sub>) was one of the main corrosion medium in the oil and gas field. In typical wet conditions, CO<sub>2</sub> can produce carbonic acid reaction, leading to the corrosion of steel. Previous studies showed [1-3] that under the same pH as in HCl solution, the steel corrosion is even more serious in H<sub>2</sub>CO<sub>3</sub> solution. Because of abundant resources and low prices, carbon steel had become the most commonly used engineering materials. However, poor corrosion resistance makes the carbon steel corrosion an urgent issue to solve. In order to reduce losses caused by corrosion, many researchers have tried a number of anti-corrosion approaches, such as reasonable anti-corrosion design, electrochemical protection, corrosion resistant materials, addition of inhibitor in the corrosive medium, etc. Among these approaches, inhibitor is a commonly used anti-corrosion material thanks to its simplicity in equipment and use, low cost, effectiveness as well as wide sources. Therefore, inhibitor

anti-corrosion technology has been widely used in oil and gas fields. Nevertheless, many chemical synthetic inhibitors were poisonous, which are harmful to human body in production process or usage, and can also cause serious environmental problems [4].

With the increase of awareness for environmental protection, green chemistry has gained more and more attention. Because of abundant raw material, low cost, renewable resources and being generally nontoxic, plant extracts have a great research prospects as corrosion inhibitors. So far, a few plant extracts have been reported as corrosion inhibitors, such as Marigold flower [5], bamboo leave [6], rice bran [7], licorice [8], Mansoa alliacea [9], Gingko biloba [10], Musa paradisica peel [11], Lupine [12], etc. The plant extracts are mostly composed of aldehydes, amines, carboxylic acids and heterocyclic compounds that have polar groups (consisting of N, O, S. etc.) with high electronegativity, and have shown good inhibition in reported studies [13], leading to the growing interest in the exploration of alternative environmentally friendly inhibitors with lower cost and better effect.

Tangerine peel (TP), also known as orange peel, is Rutaceae citrus obtained from the dried orange peel [14]. TP has a long history as medicinal and edible resource in China, with great abundance in resources as well as wide planting area and high yields. TP can regulate qi-flowing for strengthening spleen, removing fishy solution grease and crab poison. TP contains numerous natural organic compounds, such as flavonoids, organic acids, pectin, dietary fiber, polysaccharides and trace elements [15], which makes it structurally suitable as environment-friendly corrosion inhibitors.

Considering the fairly amount needed in effective protection, it is the importance of this paper to investigate the inhibition effect of the TP extract, rich in productions locally, as another source of green inhibitor for steel anti-corrosion. Electrochemical analysis were employed to investigate the corrosion inhibition efficiency, using a J55 steel sample in CO<sub>2</sub>-saturated 3.5 wt. % NaCl solution. To the best of our knowledge, TP as a corrosion inhibitor has not been reported.

## 2. EXPERIMENTAL

### 2.1 Preparation of the plant extract

TP was obtained from Sichuan province, China. First, 20 g of powdered TP was soaked in 200 mL of absolute ethyl alcohol for 48 h, followed by magnetic stirring for 2 h at 75 °C under refluxing. After the solution was cool, vacuum filtration was carried out for three times using a circulating water type vacuum pump. Excess ethanol was removed by rotary evaporation. The refluxed solution was filtered and concentrated to 100 mL. This solution was used to study the corrosion inhibition properties.

### 2.2 Characterization of TPE

FTIR was done on a Nicolet 6700 infrared spectrometer controlled by the Omnic software at wavenumber ranges from 400 to 4000 cm<sup>-1</sup> using KBr disk as the sample holder. The characterization was used to determine whether TPE is compositionally possible for use as a corrosion inhibitor.

### 2.3 Electrochemical measurements

The composition (wt. %) of the J55 steel specimen is: C 0.24%, Si 0.22%, Mn 1.1%, P 0.103%, S 0.004%, Cr 0.5%, Ni 0.28%, Mo 0.021%, Cu 0.019% and balance Fe. The size of the sample used for electrochemical studies is 70 mm × 10 mm × 3 mm (L×W×H). The work surface of each specimen steel sheet was sequentially subjected to polishing, degreasing with ethanol and acetone, and drying. Finally the specimen was encapsulated with epoxy resin, leaving only an area of 1 cm<sup>2</sup> exposed as the electrode (WE).

Electrochemical measurements were implemented with an AUTOLAB PGSTAT302N electrochemical workstation, including the NOVA1.10.4 software for potentiodynamic polarization and Electrochemical Impedance Spectroscopy (EIS) measurements. All of the electrochemical experiments were conducted using a conventional three-electrode cell system, where the J55 steel was used as working electrode (WE). A saturated calomel electrode and a platinum electrode were used as the reference electrode (RE) and the counter electrode (CE), respectively. The WE was immersed in test solution at open circuit potential (OCP) for 30 minutes before the electrochemical tests. The polarization curves were obtained at a scan rate of 1 mV s<sup>-1</sup> in the potential range of -300 mV to +300 mV. Electrochemical impedance spectroscopy (EIS) measurements were carried out under potentiostatic conditions over a frequency range from 0.01 Hz to 100 kHz with an amplitude of 10 mV on the AC signal.

### 2.4 Scanning electron microscopy (SEM) and energy dispersive spectroscopy (EDS)

Morphological changes on the sample surface can reflect the effect of corrosion and inhibition. After electrochemical test, the J55 steel electrodes were naturally dried in ambient condition. Micrographs of the J55 steel surface and those with and without the addition of inhibitor were recorded using a ZEISS EVO MA15 SEM. The element content of steel surface was analyzed by EDS hyphenated with SEM.

### 2.5 Contact angle analysis (CAA)

The contact angle shows the infiltration degree of the solution to the steel sheet. A larger value of the contact angle shows a greater inhibition effect of the material on steel corrosion. The specimens were pretreatment by the test solution with and without TPE at different concentrations. The contact angle analysis was performed on a JGW-360A instrument. Sample dimension is 30 mm × 10 mm × 2 mm.

### 2.6 Weight loss experiment

To study the effect of temperature on the inhibition efficiency of TPE, the weight loss experiment was carried out by Hanging slices method. The test solution is a CO<sub>2</sub> saturated 3.5 wt. % NaCl solution containing 1% v/v of TPE. The experiment temperature was set to 40 °C, 50 °C, 60 °C,

70 °C and 80 °C. At each temperature, three parallel samples were analyzed. The corrosion time was 72 h. After the weight loss experiment, the corrosion morphology of the samples was observed by stereo microscope.

### 3. RESULTS AND DISCUSSION

#### 3.1 Characterization of TPE

The reflection FTIR spectrum of TPE is shown in Fig. 1. The strong absorption wide peaks at 3415  $\text{cm}^{-1}$  and 3297  $\text{cm}^{-1}$  are attributed to the overlap of the N-H, O-H and the unsaturated C-H stretching vibration peak. The absorption peak at 1637  $\text{cm}^{-1}$  and 1617  $\text{cm}^{-1}$  is due to overlap between the C=C, C=O stretching vibration peak and N-H vibration peak bend of amines or amides, aromatic. The strong absorption peak at 1400  $\text{cm}^{-1}$  is attributable to overlap between C-H in-plane bend stretching and O-H bending modes of carboxylic acid or alkenes. The peaks at 1255  $\text{cm}^{-1}$  and 1054  $\text{cm}^{-1}$  are attributed to the bending vibration of C-N and C-O, respectively. The absorption peaks in the range of 1600  $\text{cm}^{-1}$  to 1000  $\text{cm}^{-1}$  also can be classified as the stretching vibration of benzene rings or miscellaneous aromatic ring skeletons.

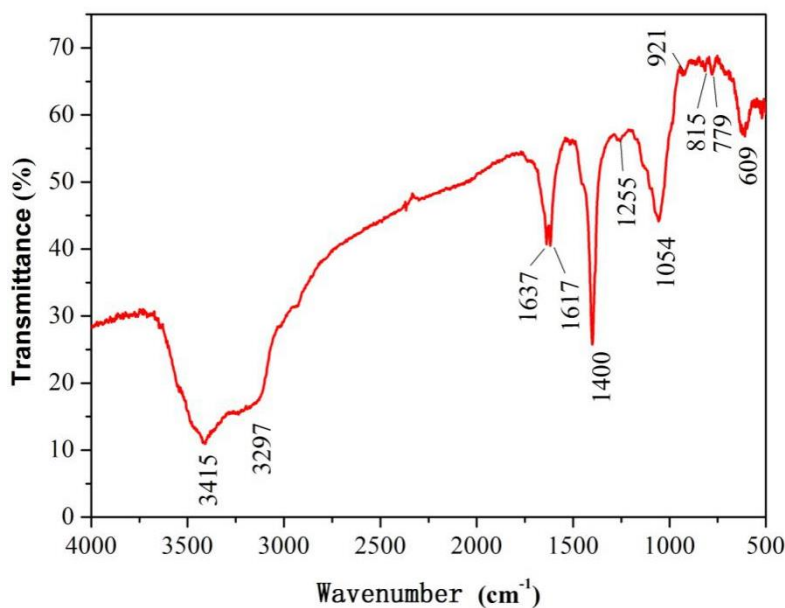


**Figure 1.** FTIR spectra of the TPE

The peaks below 1000  $\text{cm}^{-1}$  are the replaced fingerprint region of benzene rings or miscellaneous aromatic rings [16]. From the above analysis, it can be inferred that TPE contains nitrogen and oxygen atoms in functional groups (such as C=O, N-H, C=C O-H, C-O, C-N. etc.) and aromatic ring to ensure its potential to act as a corrosion inhibitor [17-20], because these groups are often considered to be the key components in corrosion protection. The reason is that N and O atoms in

these polar groups are relatively more electronegative and have lone pair electrons to supply electrons to the empty d orbitals of the Fe atoms on the sample surface, and to adsorb on the metal surface. In addition, the material containing polar groups can be adsorbed on the metal surface by electrostatic attraction. For TPE in this study, the double bond in compound can also facilitates the deposition of the extract on the metal surface [21], which further improves the interaction hence the inhibition effect.

### 3.2 Electrochemical measurements analysis

#### 3.2.1 Electrochemical impedance spectroscopy (EIS)

The Nyquist plots of J55 steel are shown in Fig. 2. The corrosion behavior of J55 steel in different corrosion solution was investigated by EIS. It can be seen that the diameter of the Nyquist plots increased after addition of TPE in the NaCl solution. The Nyquist plots contain one capacitive loop in the high frequency (HF) zone and one inductive loop in the lower frequency (LF) zone. With the increase of the TPE concentration, the diameter of the capacitance arc semicircle increases gradually, which indicates that the charge transfer resistance increased and corrosion resistance raised, leading to the gradual decrease of the corrosion rate of J55 steel. According to literature [22], the presence of the inductive loop in LF zone indicates the dissolution of iron in anode. In other words, even if molecular inhibitors of TPE are adsorbed on J55 steel, forming films, corrosion of the specimen in solution cannot be completely prevented. It also can be seen from Fig. 2 that with the addition of TPE, the change of the shape of impedance curve is very small, which indicates that the addition of TPE has no effect on the corrosion mechanism of J55 steel in the solution.

With the ZsimpWin 3.10 software, the data of Nyquist plots are fitted using the equivalent circuit, which is shown in Fig. 3, where  $R_s$  is the solution resistance and CPE is the film capacity,  $R_{ct}$  is the charge transfer resistance,  $L$  and  $R_L$  is the inductive reactance element. Inhibition efficiency ( $\eta$  %) was evaluated using the following formula:

$$\eta = \frac{R_{ct(inh)} - R_{ct}}{R_{ct(inh)}} \times 100\% \quad (1)$$

where  $R_{ct}$  and  $R_{ct(inh)}$  ( $\Omega \cdot cm^2$ ) are charge transfer resistance for J55 steel in the test solution without and with TPE, respectively. The electrochemical impedance parameter and inhibition efficiency ( $\eta$  %) are listed in Table 1.

With the increase of TPE concentration, both the charge transfer resistance  $R_{ct}$  and the inhibition efficiency of TPE are enhanced [23]. Based on the calculated results, TPE shows a greatest inhibition efficiency of 82.1% for J55 steel in the test solution at a concentration of 4% v/v, which clearly confirms its inhibition effect.

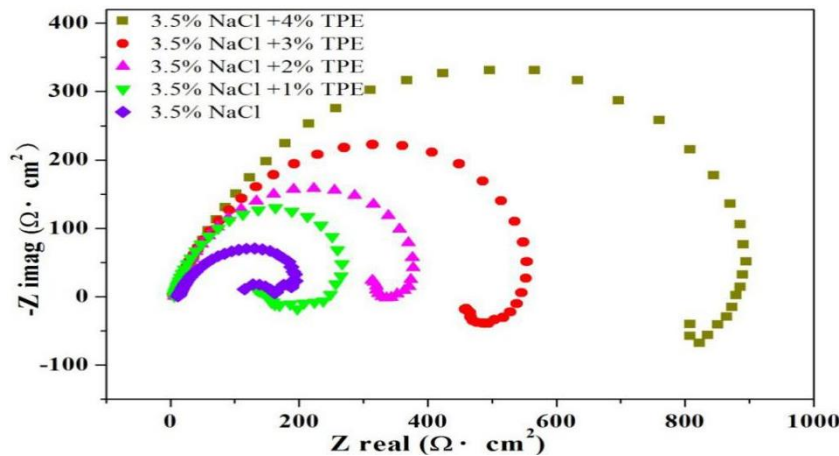


**Figure 2** Nyquist plots for J55 Steel in CO<sub>2</sub>-saturated 3.5 wt. % NaCl solution with different concentration of TPE at 25 °C

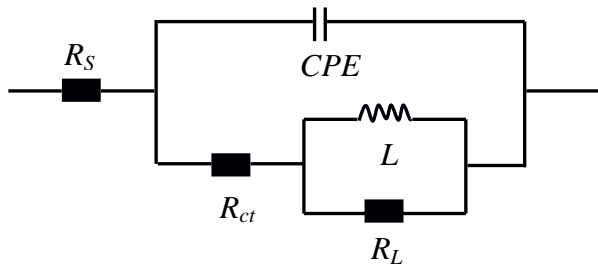


**Figure 3.** The equivalent circuit used for fit the impedance data, record for J55 steel in CO<sub>2</sub>-saturated 3.5 wt. % NaCl solution in the presence of TPE

**Table 1.** EIS parameters for J55 steel in CO<sub>2</sub>-saturated 3.5 wt. % NaCl solution with different TPE concentrations

Concentration (% v/v)	$R_s$ ( $\Omega \cdot \text{cm}^2$ )	$10^4 CPE$ ( $\text{F} \cdot \text{cm}^{-2}$ )	$R_{ct}$ ( $\Omega \cdot \text{cm}^2$ )	$n$	$L$ ( $\text{H} \cdot \text{cm}^2$ )	$R_L$ ( $\Omega \cdot \text{cm}^2$ )	$\eta$ (%)
0	7.668	8.106	150.5	0.6966	75.19	59.64	-
1	5.664	6.845	258.8	0.7440	65.68	140.5	41.8
2	6.742	4.755	330.7	0.7971	94.51	108.7	54.5
3	7.209	3.132	473.9	0.8386	165.2	274.6	68.2
4	8.193	2.685	842.5	0.8951	552.8	210.8	82.1

### 3.2.2 Polarization curves

The polarization curves for J55 steel at different concentration of TPE in CO<sub>2</sub>-saturated 3.5 wt. % NaCl solution are shown in Fig. 4. By using the Tafel linear extrapolation method, the polarization curves are fitted and some important parameters are obtained, including the anodic Tafel slope ( $b_a$ ), cathode Tafel slope ( $b_c$ ), the corrosion current density ( $I_{corr}$ ) and the corrosion potential ( $E_{corr}$ ) that are summarized in Table 2. The inhibition efficiency ( $\eta$ ) is calculated as follow:

$$\eta = \frac{I_{corr} - I_{corr(inh)}}{I_{corr}} \times 100\% \quad (2)$$

where  $I_{corr}$  and  $I_{corr(inh)}$  represents the corrosion current density value in solution without and with TPE, respectively.

**Table 2.** Polarization parameters and inhibition efficiency for J55 steel in CO<sub>2</sub>-saturated 3.5 wt. % NaCl solution with different TPE concentrations

Concentration (% v/v)	$E_{corr}$ (mV)	$I_{corr}$ ( $\mu\text{A}\cdot\text{cm}^{-2}$ )	$b_a$ (mV·decade $^{-1}$ )	$b_c$ (mV·decade $^{-1}$ )	$\eta\%$
0	-751	45.88	66	509	-
1	-747	25.41	72	313	44.6
2	-729	20.60	65	487	55.1
3	-748	12.47	121	345	70.6
4	-724	7.66	103	359	83.3

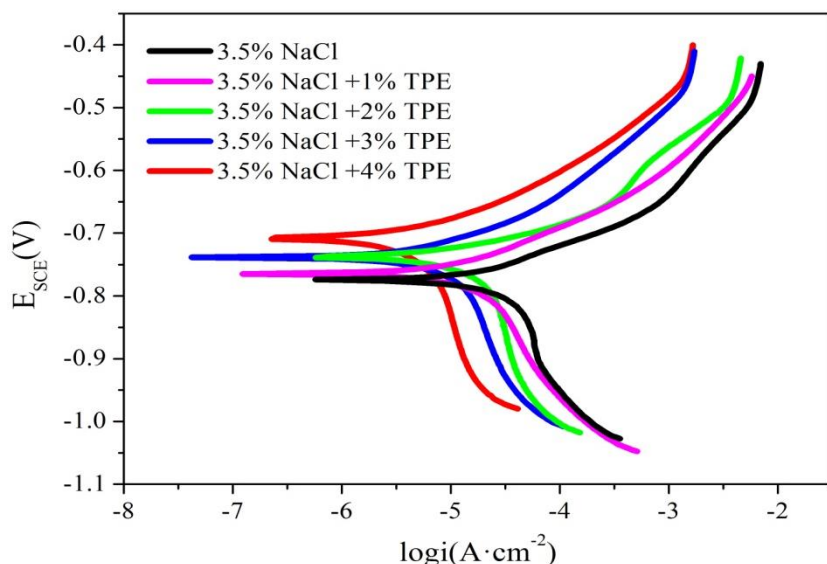


**Figure 4.** Polarization curves of J55 steel in CO<sub>2</sub>-saturated 3.5 wt. % NaCl solution with different TPE concentrations at 25°C

It is clear from Table 2 that the corrosion current density ( $I_{corr}$ ) of J55 steel decreases obviously after the addition of corrosion inhibitor, and the corrosion potential ( $E_{corr}$ ) of J55 steel moves slightly to the anode. Generally, a corrosion inhibitor can be defined as anodic or cathodic type if the shift of corrosion potential is more than 85 mV [24-25] after adding corrosion inhibitor. With the addition of the inhibitor, the change of  $E_{corr}$ , about 4-27 mV, is less than 85 mV, which suggests that TPE acts as a mixed-type inhibitor where the anode inhibition is primary. Along with the increase of TPE concentration, the inhibition efficiency ( $\eta$ ) is raised. The maximum inhibition efficiency exhibited by TPE for J55 steel corrosion in test solution was 83.3%, which agrees well with the result of the EIS test.

In order to further clarify the type of TPE inhibitor, the anode reaction coefficient ( $f_a$ ) and the cathode reaction coefficient ( $f_c$ ) of TPE on J55 steel, shown in Table 3, are calculated based on the parameters from Table 2 using formula (3) and (4) [26]:

$$f_a = \frac{I_{corr(inh)}}{I_{corr}} \exp\left(\frac{E_{corr} - E_{corr(inh)}}{b_a}\right) \quad (3)$$

$$f_c = \frac{I_{corr(inh)}}{I_{corr}} \exp\left(\frac{E_{corr(inh)} - E_{corr}}{b_c}\right) \quad (4)$$

where  $E_{corr}$  and  $E_{corr(inh)}$  stands for the corrosion potential without and with inhibitor, whereas  $I_{corr}$  and  $I_{corr(inh)}$  represents the corresponding corrosion current density, respectively.

Singh et al. [27] reported that the inhibitor would have a certain inhibitory effect on the electrode reaction if the reaction coefficient is less than 1. For the same inhibitor, the smaller the value of reaction coefficient is better the inhibition effect of inhibitor on the electrode. As can be seen from Table 3, the anode reaction coefficient  $f_a$  and the cathode reaction coefficient  $f_c$  are both smaller than 1. Along with the increment of the concentration of TPE, the gradual decrease of  $f_a$  and  $f_c$  indicates that the inhibitory effect of TPE on the anode and cathode reaction was gradually enhanced with the increase of TPE content. The ratio of  $f_a/f_c$  is slightly smaller than 1, which suggests that the inhibitory effect of the TPE on the anodic reaction is a little better, and the TPE can be considered to act as a mixed-type inhibitor. This result is in agreement with the fact that the corrosion potential shift of J55 steel obtained by polarization curve is less than 85 mv.

**Table 3.** Reaction coefficient of TPE on J55 steel in CO<sub>2</sub>-saturated 3.5 wt. % NaCl solution with different TPE concentration at 25°C

Concentration (% v/v)	$f_a$	$f_c$	$f_a/f_c$
1	0.5239	0.5309	0.9808
2	0.4129	0.4169	0.9904
3	0.2651	0.2702	0.9811
4	0.1285	0.1299	0.9892

### 3.3 Surface analysis

#### 3.3.1 Scanning electron micrographs (SEM)

Figure 5 illustrates the surface corrosion morphologies of J55 steel specimen without and with 4% v/v of TPE after electrochemical test. It can be seen that the surface of the steel sample exposed in the corrosion solution without inhibitor (Fig 5a) is very rough and the corrosion product is thick. However, the surface of the steel sample exposed in the corrosion solution with inhibitor becomes

smoother, with only a small amount of corrosion products attached to the surface, which indicates that the TPE inhibitor molecules are adsorbed on the surface of J55 steel, slowing down the corrosion of J55 steel in the CO<sub>2</sub>-saturated NaCl solution. This result is also consistent with the conclusion from the electrochemical experiments.

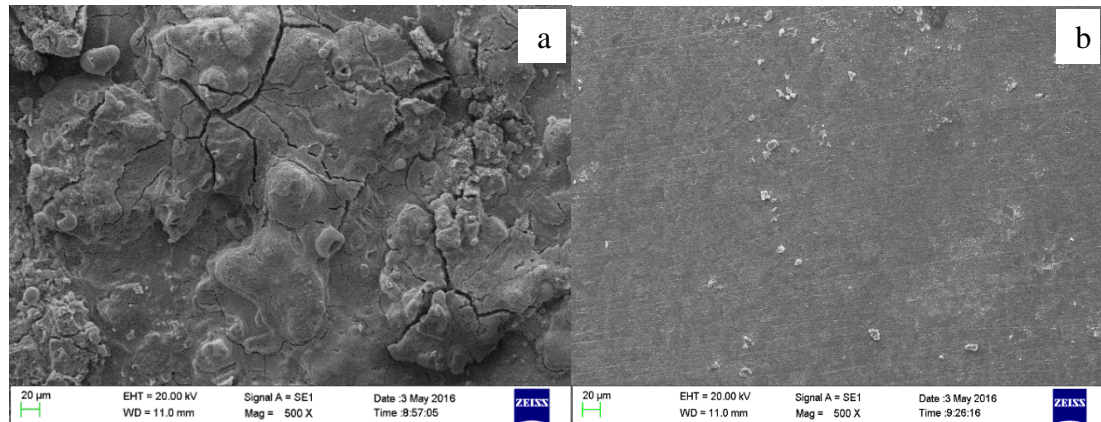


**Figure 5.** SEM micrographs of J55 steel in CO<sub>2</sub>-saturated 3.5 wt. % NaCl solutions, (a) without, and (b) with 4% v/v TPE inhibitor

### 3.3.2 Energy disperse spectroscopy (EDS)

The EDS of the surface of J55 steel specimen without and with 4% v/v of TPE are shown in Fig. 6, and the corresponding element contents are summarized in Table 4. It is seen that without TPE, the content of Fe is lower, whereas the content of C and O is higher. Element Cl also exists on the J55 steel surface, which indicates that the corrosion occurs on J55 steel because of the Cl<sup>-</sup> in corrosion solution and CO<sub>2</sub> dissolved in water. With the addition of 4% v/v TPE to the solution, the content of Fe increases and that of C and O decreases, whereas element Cl disappears on the specimen surface, which indicates that the TPE slows down the corrosion behavior of J55 steel. This result is consistent with the result from the SEM where only little corrosion products were found for steel specimen with TPE.

**Table 4.** Content of elements on J55 steel surface after electrochemical analysis

Concentration (% v/v)	C (wt. %)	O (wt. %)	Cl (wt. %)	Mn (wt. %)	Fe (wt. %)	Au (wt. %)
0	2.56	9.73	0.87	-	68.48	18.36
4	1.58	0.38	-	1.36	81.59	15.09

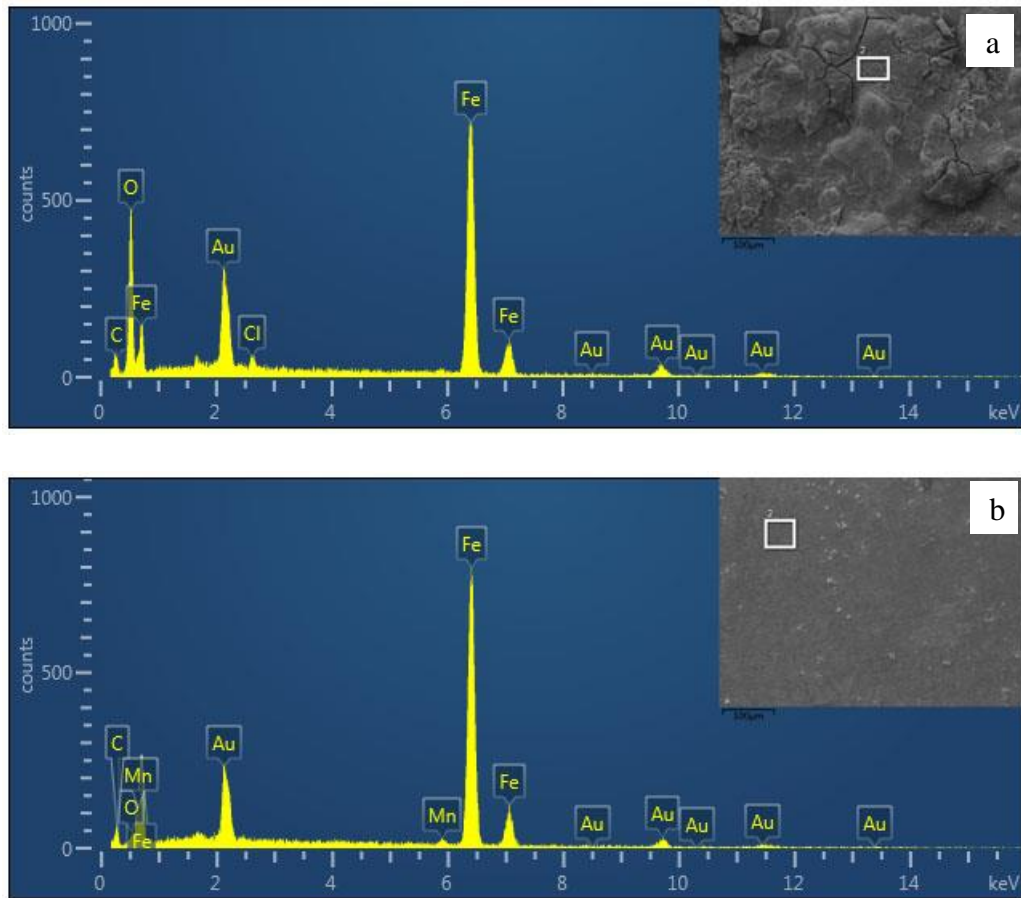


**Figure 6.** EDS of J55 steel after electrochemical analysis in CO<sub>2</sub>-saturated 3.5 wt. % NaCl solution, (a) without, and (b) with 4% v/v TPE inhibitor.

### 3.4 Contact angle (CA) analysis

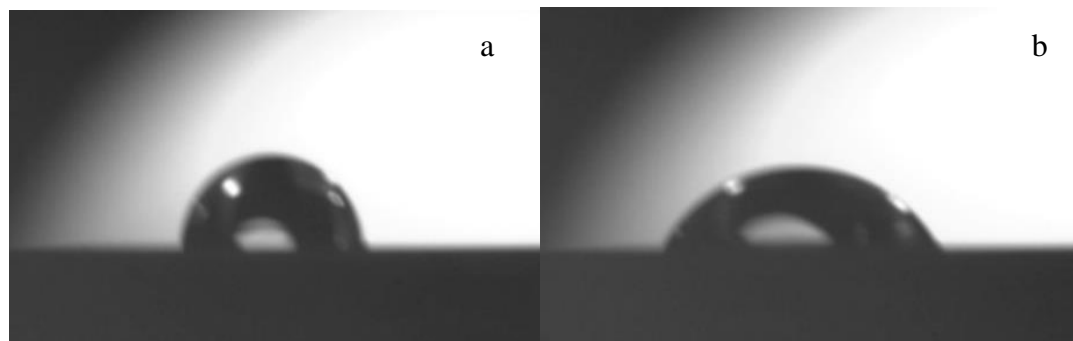


**Figure 7.** Contact angle analysis between different test solutions and J55 steel surface. (a) 4% v/v TPE: 81.55°, (b) 0% v/v TPE: 61.99°

Figure 7 presents the CA between the J55 steel surface and the CO<sub>2</sub>-saturated 3.5 wt. % NaCl solution containing different concentration of TPE. The relationship between the TPE concentration and the contact angle are shown in Fig. 8. With the increase of TPE concentration, the CA of J55 steel increases gradually, which shows that the wettability between the corrosion solutions and the surface

of sheet steel are gradually reduced. It is also believed that the contact area between the two interfaces is gradually decreased, leading to reduce of the corrosion of J55 steel in the solution.

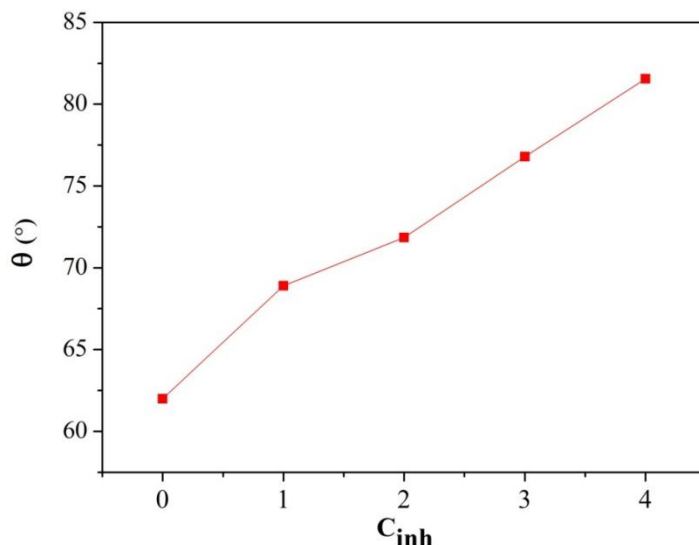


**Figure 8.** Variation of contact angle of J55 steel surface to the 3.5% NaCl solution with different inhibitor concentration

### 3.5 Weight loss experiment

Figure 9 shows the stereo microscope image of J55 steel after weight loss experiment under different temperature.

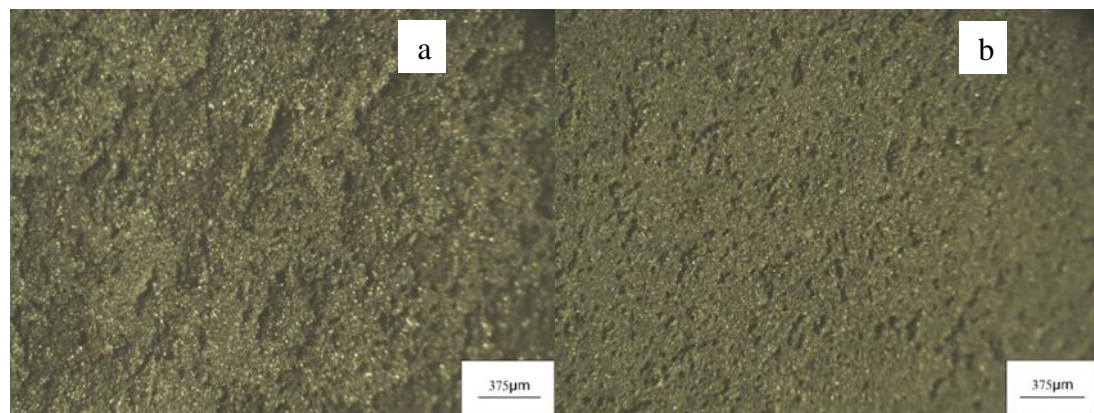


**Figure 9.** Microscope image of J55 steel at (a) 80°C (b) 40°C in CO<sub>2</sub>-saturated 3.5 wt. % NaCl solution containing 1 % v/v TPE

By using formula (5), the corrosion rate of the sample at the experimental temperature can be calculated based on the average corrosion rate of the three parallel samples:

$$V = \frac{W_0 - W_t}{St} \quad (5)$$

where  $V$  ( $\text{g}/(\text{m}^2 \cdot \text{h})$ ) is the corrosion rate of steel sheet,  $W_0$  ( $\text{g}$ ) is the initial weight of steel sheet,  $W_t$  ( $\text{g}$ ) is the weight of the steel sheet after removal of corrosion products,  $S$  ( $\text{m}^2$ ) is surface area of steel sheet and  $t$  ( $\text{h}$ ) is the duration time of corrosion. The inhibition efficiency ( $\eta$ ) is calculated as follow:

$$\eta = \frac{V_0 - V_{inh}}{V_0} \quad (6)$$

where  $V_0$  ( $\text{g}/(\text{m}^2 \cdot \text{h})$ ) and  $V_{inh}$  ( $\text{g}/(\text{m}^2 \cdot \text{h})$ ) stands for the corrosion rate of steel sheet without and with TPE, respectively. The corrosion rate and the inhibition efficiency at different temperatures are listed in Table 5.

**Table 5.** Corrosion rate of J55 steel and the inhibition efficiency of TPE at different temperatures

$T$ ( $^\circ\text{C}$ )	$t$ ( $\text{h}$ )	$c$ (v/v %)	$V$ ( $\text{g} \cdot \text{m}^{-2} \cdot \text{h}^{-1}$ )	$\eta$ (%)
40 °C	72	0	3.513	-
		1	2.142	39.0
50 °C	72	0	5.699	-
		1	3.701	35.1
60 °C	72	0	8.295	-
		1	5.558	32.9
70 °C	72	0	12.013	-
		1	8.619	28.3
80 °C	72	0	15.723	-
		1	11.762	25.2

It is seen from Table 5 that with the increase of experimental temperature at the same TPE concentration, the corrosion rate of J55 steel increases and the inhibition effect becomes weak. The reason for this phenomenon may be that the elevated temperature is not conducive to the adsorption of TPE molecules on J55 steel surface. The desorption rate of the inhibitor molecules is greater than their adsorption rate, which results in the decrease of the number of the inhibitor molecules on the J55 steel surface, and thus makes the corrosion rate of J55 steel accelerated and the inhibition effect for corrosion decreased. In addition, this phenomenon indicates that the inhibition effect of TPE is largely affected by the experimental temperature. Another reason may be that the raised temperature deusters the effective inhibitor component of TPE, thereby reducing the effect of the corrosion inhibition.

### 3.6. Adsorption isotherm

The basic information about the interaction of inhibitor molecules on the metal surface can be obtained by using the adsorption model. In order to obtain the adsorption model of corrosion inhibitor on the metal surface, it is necessary to acquire the function between the surface coverage degree ( $\theta$ ) of

the inhibitor on the sample surface and the inhibitor concentration ( $c$ ). Four types of relevant adsorption model can be expressed by the following equations [28-29]:

$$\frac{c}{\theta} = \frac{1}{k_{ads}} + c \text{ (Langmuir isotherm)} \quad (7)$$

$$e^{-2a\theta} = k_{ads} \cdot c \text{ (Temkin isotherm)} \quad (8)$$

$$\log \theta = \log k_{ads} + n \log c \text{ (Freundlich isotherm)} \quad (9)$$

$$\frac{\theta}{1-\theta} e^{-2a\theta} = k_{ads} \cdot c \text{ (Frumkin isotherm)} \quad (10)$$

where  $c$  is the inhibitor concentration,  $K_{ads}$  is the equilibrium constant of adsorption and  $\theta$  denotes the degree of surface coverage. In the present work, the adsorption behavior of TPE on J55 steel surface is analyzed by using the impedance parameters obtained by the fitting of EIS, and the degree of surface coverage ( $\theta$ ) is calculated by the following equation [30]:

$$\theta = \frac{R_{ct(inh)} - R_{ct}}{R_{ct(inh)}} \quad (11)$$

where  $R_{ct(inh)}$  and  $R_{ct}$  ( $\Omega \cdot \text{cm}^2$ ) stands for the charge transfer resistance for J55 steel without and with inhibitor, respectively. The calculated results are listed in Table 6.

**Table 6.** Degree of surface coverage ( $\theta$ ) for J55 steel in CO<sub>2</sub>-saturated 3.5 wt. % NaCl solution with different TPE concentrations

Concentration (% v/v)	$R_{ct}$ ( $\Omega \cdot \text{cm}^2$ )	$\theta$
0	150.5	-
1	258.8	0.418
2	330.7	0.545
3	473.9	0.682
4	842.5	0.821

The Langmuir, Temkin, Freundlich and Frumkin isotherm are adopted to fit the experiment data. The results show that only the Langmuir adsorption plot has a relatively higher linear correlation coefficient [31]. The fitting graph is shown in Fig. 10. The best straight line is obtained with a linear correlation coefficient of 0.99683, indicating that the adsorption behavior of TPE on the surface of J55 steel follows the Langmuir isotherm. The slopes is 0.98, which is very close to 1, suggesting that the absorption of TPE on J55 steel samples is monolayer adsorption where there is no interaction among the adsorbed inhibitor molecules, and the chance of each inhibitor molecule adsorbing at any position on the J55 steel surface is almost equal to each other [32].

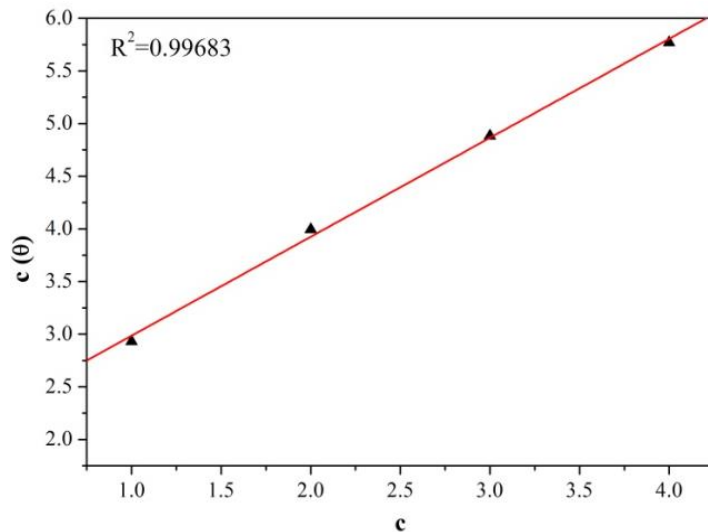


**Figure 10.** Langmuir adsorption isotherm plots for EIS at different TPE concentrations

### 3.7 Adsorption thermodynamics

The calculated Gibbs free energy ( $\Delta G^\theta$ ) of the adsorption process can be used to analyze whether the adsorption process of the inhibitor molecules on the sample surface is spontaneous or not. The equilibrium constant ( $K_{ads} = 0.51$ ) of J55 steel at 25°C was obtained by using the Langmuir isotherm. The Gibbs free energy can be calculated using the following equation [33]:

$$\log k_{ads} = -\log C_{H_2O} - \frac{\Delta G^\theta}{2.303RT} \quad (12)$$

where  $C_{H_2O}$  (1000 g/L) is the concentration of water,  $R$  (8.31 J/mol·K) is the molar gas constant,  $T$  (k) denotes the thermodynamic temperature and  $K$  is the standard equilibrium constant. Based on equation (12) and the value of  $K_{ads}$  of J55 steel, the Gibbs free energy ( $\Delta G^\theta$ ) of J55 steel is calculated to be -8.28 KJ/mol, which is less than zero, suggesting that the adsorption behavior of TPE molecules on the J55 steel surface is a spontaneous process. Generally, if the value of  $\Delta G^\theta$  is between -20 and 0, the adsorption of inhibitor molecules on the sample surface would be physical adsorption, whereas if the value of  $\Delta G^\theta$  is less than -40, the adsorption would be considered as chemical adsorption [34]. According to the value of  $\Delta G^\theta$  of J55 steel, the adsorption processes of TPE on the J55 steel surface is considered to be spontaneous physical adsorption processes, and thus slows down the corrosion of J55 steel in the CO<sub>2</sub>-saturated 3.5 wt. % NaCl solution.

### 3.8 Adsorption dynamics

EIS data are used to study the adsorption dynamics of corrosion inhibitor molecules on the surface of J55 steel. Combined with the dynamics model proposed by El-Awady [35] et al., the fitted result is shown in Fig. 11. The dynamic model adopted is as follows:

$$\lg \frac{\theta}{1-\theta} = y \lg c + \lg K' \quad (13)$$

where  $\theta$  is the degree of surface coverage,  $c$  (% v/v) is the inhibitor concentration,  $K'$  is the equilibrium constant and  $y$  is the number of inhibitor molecules adsorbed on an active site of the J55 steel surface.

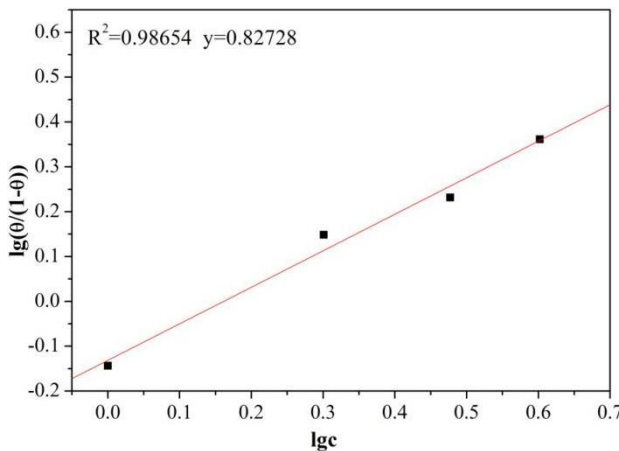


**Figure 11.** Curve fitting of TPE by El-Awady dynamic model

It can be seen that the linear correlation coefficient of J55 steel is 0.98654 and the slope ( $y$ ) value is 0.82728. The linear correlation coefficient is close to 1, indicating the adsorption of TPE on the surface of the J55 steel conforms to the El-Awady dynamic model. The adsorption morphology of adsorbed molecules can be determined by the  $y$  value. If the  $y$  value is more than 1, a number of inhibitor molecules would be adsorbed on an active spot of the steel surface, which is multi-molecular adsorption. When the  $y$  value is less than 1, the number of inhibitor molecules adsorbed on an active spot would be less than 1, corresponding to the monolayer adsorption [36]. The  $y$  value of J55 steel is 0.82728, suggesting that the absorption of TPE on J55 steel is a monolayer adsorption. This result is consistent with what was concluded using the Langmuir isothermal adsorption model.

#### 4. CONCLUSION

The corrosion inhibition effect of the tangerine peel extract on J55 steel in a  $\text{CO}_2$ -saturated 3.5 wt. % NaCl solution was investigated by electrochemical, surface analysis and Potentiodynamic. FTIR spectrum confirms that TPE is compositionally promising to be a steel corrosion inhibitor. EIS, Polarization curves, SEM, EDS and contact angle analysis indicate that TPE acts as a mixed-type inhibitor that slows down the corrosion rate of J55 steel in the  $\text{CO}_2$ -saturated 3.5 wt. % NaCl solution. The inhibition efficiency of TPE increases with the increase of the inhibitor concentration, while somehow decreases when temperature increases. Particularly, when the inhibitor concentration is merely 4% v/v, the inhibition efficiency of TPE can be as high as 82.1% (EIS) and 83.3% (Tafel). The adsorption of TPE on J55 steel surface in the form of monolayer is a spontaneous physical process, with characteristics that are fit to the Langmuir isothermal absorption model and the El-Awady dynamic model. These findings support that TPE can act as a good inhibitor for J55 steel in the  $\text{CO}_2$ -saturated 3.5 wt. % NaCl solution. This study contributes to the demanding exploration of

environmentally friendly inhibitor concerning steel pipe corrosion and provides alternative means of material protection.

## ACKNOWLEDGEMENTS

This work was financially supported by the National Natural Science Foundation of China (No. 51374180), the Key Lab of Material of Oil and Gas Field (No. X151516KCL23). The authors acknowledge a research funding from the Education Department of Sichuan Province (No. 17ZA0419), as well as start-up funding from Southwest Petroleum University.

## References

1. A. S. Yaroa, K. R. Abdul-Khalika and A. A. Khadomb, *J. Loss. Prevent. Proc.*, 38 (2015) 24.
2. S. L. Wu, Z. Z. Cui and C. F. Li, *J. Chin. Soc. Corros. Prot.*, 23 (2003) 340.
3. G. M. Li, L. W. Liu and J. S. Zheng, *J. Chin. Soc. Corros. Prot.*, 20 (2000) 205.
4. M. M. Solomon, S. A. Umoren, I. I. Udosoro and A. P. Udoh, *Corros. Sci.*, 52 (2010) 1317.
5. P. Mourya, S. Banerjee and M. M. Singh, *Corros. Sci.*, 85 (2014) 352.
6. L. Li, X. Zhang, J. Lei, J. He, S. Zhang and F. Pan, *Corros. Sci.*, 63 (2012) 82.
7. D. Liu, Y. H. Lin, Y. G. Ding and D. Z. Zeng, *Anti. Corros. Meth. Mater.*, 58 (2011) 205.
8. M. A. Deyab, *J. Ind. Eng. Chem.*, 22 (2015) 384.
9. F. Suedile, F. Robert, C. Roos and M. Lebrini, *Electrochim. Acta.*, 133 (2014) 631.
10. G. Chen, M. Zhang, J. R. Zhao, Z. Meng and J. Zhang, *Chem. Central. J.*, 7 (2013) 1.
11. G. Ji, S. Anjum, S. Sundaram and R. Prakash, *Corros. Sci.*, 90 (2015) 107.
12. A. M. Abdel-Gaber, B. A. Abd-El-Nabey and M. Saadawy, *Corros. Sci.*, 51 (2009) 1038.
13. M. A. Quraishi, A. Singh, V. K. Singh, D. K. Yadav and A. K. Singh, *Mater. Chem. Phys.*, 122 (2010) 114.
14. Q. He and K. J. Xiao, *J. Food Control*, 69 (2016) 339.
15. A. M. Rincón, A. M. Vásquez and F. C. Padilla, *Arch Lationam Nurt.*, 55 (2005) 305.
16. X. H. Li, H. Fu and S. R. Deng, *J. Chin. Soc. Corros. Prot.*, 31 (2011) 149.
17. G. Ji, S. Anjum, S. Sundaram, and R. Prakash, *Corros. Sci.*, 90 (2015) 107
18. M. Lebrini, F. Robert and C. Roos, *Int. J. Electrochem. Sci.*, 5 (2010) 1698
19. V. Rajeswaria, D. Kesavanb and M. Gopiramanc, *Appl. Surf. Sci.*, 314 (2014) 537.
20. G. Ji, S. Anjum, S. Sundaram and R. Prakash, *Corros. Sci.*, 90 (2015) 107.
21. B. Huang, Y. Lin and A. Singh, et al. *Anti-Corros. Method. M.*, 62 (2015) 388.
22. M. D. Zhang, C. N. Cao and H. C. Lin, *J. Chin. Soc. Corros. Prot.*, 13 (1993) 101.
23. M. N. El-Haddad and A. S. Fouda, *J. Mol. Liq.*, 209 (2015) 480.
24. T. Peme, L. O. Olasunkanmi, I. Bahadur, A. S. Adekunle, M. M. Kabanda and E. E. Ebenso, *Mol.*, 20 (2015) 16004.
25. M. Xia, L. P. Guan and K. Gong, *Corros. Sci. Prot. Technol.*, 25(2013) 495.
26. X. H. Li, H. Fu and S. R. Deng, *J. Chin. Soc. Corros. Prot.*, 31 (2011) 149.
27. C. N. Cao, Principles of Electrochemistry of Corrosion, (2004) BeiJing, China.
28. A. K. Satapathy, G. Gunasekaran, S. C. Sahoo, K. Amit and P. V. Rodrigues, *Corros. Sci.*, 51 (2009) 2848.
29. E. Bayol, K. Kayakırılmaz, M. Erbil, *Mater. Chem. Phys.* 104 (2007) 74.
30. X. H. Li, S. R. Deng and H. Fu, *Corros & Prot.*, 31 (2010) 287.
31. L. R. Chauhan and G. Gunasekaran, *Corros. Sci.*, 49(2007) 1143.
32. B. Xie, C. Lai and N. Zeng, *Mater. Prot.*, 45 (2012) 55.
33. E. A. Noor, *J. Appl. Electrochem.*, 39 (2009) 1465.
34. F. M. You, G. S. Wei and M. Dai, *Corros & Prot.*, 35 (2014) 1016.

35. A. A. El-Awady, B. A. Abd-El-Nabey and S. G. Aziz, *J. Chem. Soc.*, 89 (1993) 795.
36. B. G. Ateya, B. E. El-Anadouli and F. M. El-Nizamy, *Corros. Sci.*, 124 (1984) 509.

© 2017 The Authors. Published by ESG ([www.electrochemsci.org](http://www.electrochemsci.org)). This article is an open access article distributed under the terms and conditions of the Creative Commons Attribution license (<http://creativecommons.org/licenses/by/4.0/>).